Resonant focusing in a planar microcavity

Hervé Rigneault, Serge Monneret, Christoph I Westbrook

Resonant focusing in a planar microcavity

H. Rigneault

Laboratoire d'Optique des Surfaces et des Couches Minces,
Unité Associée au Centre National de la Recherche Scientifique, Ecole Nationale Supérieure de Physique de Marseille,
Domaine Universitaire de St. Jérôme, 13397 Marseille Cedex 20, France
(e-mail: herve.rigneault@enspm.u-3mrs.fr)

S. Monneret

Département de Chimie Physique des Réactions, Unité Associée au Centre National de la Recherche Scientifique,
Ecole Nationale Supérieure des Industries Chimiques de Nancy,
1 rue Grandville, B.P. 451, 54001 Nancy Cedex, France

C. I. Westbrook

Laboratoire Charles Fabry de l'Institut d'Optique, Unité Associée au Centre National de la Recherche Scientifique,
B.P. 147, 91403 Orsay Cedex, France

We study the focusing of a Gaussian laser beam in a microscopic planar cavity when the laser wavelength is resonant in the cavity but the beam divergence is larger than the acceptance angle of the cavity. Using the luminescence of implanted praseodymium ions as a microscopic probe for the total electric field inside the spacer of the microresonator, we investigate theoretically and experimentally how strong focusing alters the photoexcitation of luminescent species located inside such a structure. © 1998 Optical Society of America
[S0740-3224(98)00710-3]

OCIS codes: 180.2520, 310.6860, 260.3800.

For an increasing number of problems in modern optics it is important to understand the optical behavior of focused beams falling onto planar multilayer structures. Because the reflectivity of these microstructures may depend strongly on the angle of incidence, it is important to investigate carefully the reflected and the transmitted focused wave fronts versus the amount of power that it is possible to couple inside the stack. This point is crucial when the incident focused light is a pump exciting a luminescent species located inside a multilayer structure. Such is the case, for instance, in many experiments that investigate the control of spontaneous emission of sources located within resonant planar microcavities.[1–5] More precisely, in these experiments the luminescent species are usually located in the spacer of a Fabry–Perot-type microcavity (see Fig. 1) whose structure is chosen to have an electromagnetic resonant at the emitter wavelength λ_0 to confine the emitted light in the direction normal to the layers.[3,5] It is clear that in this case the reflectivity of the microresonator shows a strong dependence on the propagation angle at λ_0 but also at any wavelength close to λ_0. This dependence can appear when photoluminescence is studied: an incident pump beam of wavelength λ_p, usually with $\lambda_p < \lambda_0$, is focused into the microcavity at an incidence angle that optimizes the overlap between the spatial distribution of the pump light and that of the luminescent species inside the microcavity. Dye molecules,[1] rare-earth atoms,[4,5] and quantum-well[2,3] excitations are examples for which the wavelength of maximum absorption is close to the wavelength of the transition of interest. The size of the excited area and the value of the pump electric field then depend strongly on the pump focusing conditions inside the microcavity.

This paper is devoted to a theoretical and experimental of the reflected, transmitted, and internal electric fields of a focused Ar-line pump beam at $\lambda_p = 457.9$ nm incident upon a microcavity structure. This microstructure (Fig. 1) is tuned at $\lambda_0 = 490$ nm for normal incidence and enhances the spontaneously emitted light of praseodymium ions in the normal direction.[5] The ions were implanted inside the spacer of the microstructure by an ion implantation technique.[6] More precisely, the structure of the Ta_2O_5/SiO_2 microcavity of interest is glass substrate/ HLHLHLHL 2H LHLHLHLH, where H and L denote, respectively, high (Ta_2O_5) and low (SiO_2) refractive-index layers ($n_H = 2.2$, $n_L = 1.5$) whose optical thicknesses are $\lambda_0/4$. The Pr ions are located inside the 2H spacer, and the Ar pump beam excites the $^3P_0 \rightarrow {}^3H_4$ Pr transition at $\lambda_0 = 490$ nm.

Before going into the details of a strongly focused pump beam incoming onto the stack, let us consider first the simple case in which the excitation beam is close to a plane wave. This situation is approximately achieved experimentally by use of a long-focal-length lens ($f = 200$ mm), which leads to a $d = 100$ μm active spot diameter and a beam waist of $w = d/2 = 50$ μm in air. Figure 1 shows the recorded Pr luminescence intensity at λ_0 in a direction normal to the microcavity plane for various incidence angles θ of the pump beam. In the same figure, the solid curve indicates the calculated normalized
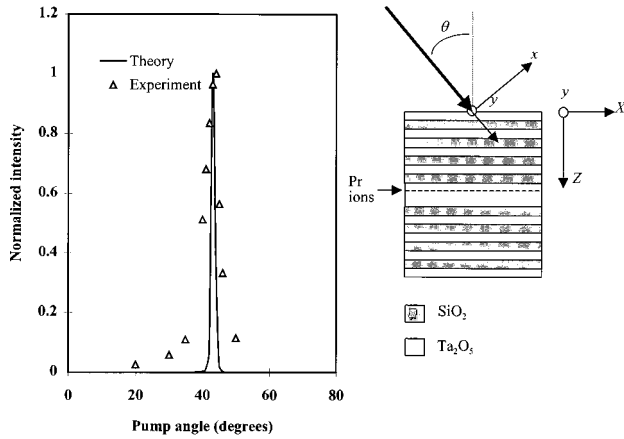
Fig. 1. Left, recorded Pr luminescence intensity at λ_0 = 490 nm in a direction normal to the microcavity versus pump angle. The theoretical curve is for plane-wave excitation. The broad wings of the experimental curve are due to the angular spread of the excitation laser. Right, microcavity design and co-ordinate frames.

average pump intensity in the microcavity spacer, assuming that the pump beam is a plane wave. The figure shows that the maximum fluorescence indeed occurs at the theoretically predicted maximum $\theta_m = 41.6°$. The experimental curve shows broader wings because of the finite angular spread of the incident pump beam.

This result demonstrates that the implanted Pr ions can be considered microscopic probes for the total pump intensity inside the microcavity spacer.[4] In the following, we use the Pr ions to investigate the coupling of a strongly focused pump beam centered about θ_m. This experimental configuration would be the natural one to use to optimize excitation of Pr ions inside the microcavity. Note that θ_m also corresponds to the optimal transmission angle for a $\lambda_p = 457.9$ nm plane wave incident upon the microcavity. Alternatively, the microcavity can be viewed as a bandpass filter near 457.9 nm for incidences near 41.6°.

Before reporting experimental results, we briefly present the electromagnetic calculations that we have implemented to compute the total focused pump electric field inside the microcavity, together with the reflected and the transmitted wave fronts. For the sake of simplicity, we restrict our analysis to the TE polarization state, where the electric field lies along the y axis.

Let us consider a Gaussian beam incident upon the cavity centered at incidence angle θ_m. This beam is focused on the plane $z = 0$ (Fig. 1), and its electric field can be written in this plane:

$$E_i(x, y, z) = E_0 \exp\left(-\frac{x^2}{w^2}\right)\exp\left(-\frac{y^2}{w^2}\right), \qquad (1)$$

where w is the incident beam waist. This field can be expanded in a familiar amplitude plane wave (PW) spectrum $W(\sigma)$:

$$E_i(x, y, 0) = \exp\left(-\frac{y^2}{w^2}\right)\int_{-\infty}^{+\infty} W(\sigma)\exp(2i\pi\sigma x)\mathrm{d}\sigma, \qquad (2)$$

where $W(\sigma) = E_0\sqrt{\pi}w\,\exp(-\pi^2 w^2\sigma^2)$, $\sigma = (\sin\theta)/\lambda_p$ is the spatial frequency, and θ is the incidence angle. The

beam power P is simply related to E_0 through $E_0{}^2 = [(4P)/(\pi w^2 Y_0)]$, with $Y_0 = \sqrt{\epsilon_0/\mu_0}$. The reflected and the transmitted powers are given by $R(\sigma)|W(\sigma)|^2$ and $T(\sigma)|W(\sigma)|^2$, respectively, where $R(\sigma)$ and $T(\sigma)$ are the intensity reflection and transmission factors of the stack. The total electric field within the microcavity at any altitude Z is given by

$$E(X, y, Z) = \exp\left(-\frac{y^2}{w^2}\right)\int_{-\infty}^{+\infty} A(\sigma, Z)\exp(2i\pi\sigma X)\mathrm{d}\sigma, \qquad (3)$$

where $A(\sigma, Z)$ is the total electric field amplitude within the stack with spatial frequency σ associated with each incident plane wave. For Eq. (3) it is assumed that the electric field remains unchanged along the y axis. This is a good approximation because the incident amplitude PW spectrum is almost unchanged by the microcavity along this axis. Furthermore, by transforming between the (x, y, z) and (X, y, Z) coordinate systems we can show[7,8] that

$$A(\sigma, Z) = \frac{1}{\cos\theta_m}\,W\left(\frac{\sigma - \sigma_m}{\cos\theta_m}\right)\widetilde{E}(\sigma, Z), \qquad (4)$$

where $\widetilde{E}(\sigma, Z)$ is the total electric field amplitude along the Z axis that results from a PW of unit amplitude incident upon the microcavity with a spatial frequency σ.

Figures 2 and 3 present some results of computation for incident pump beams at λ_p with waists $w = 10\ \mu$m (Fig. 2) and $w = 1\ \mu$m (Fig. 3). More precisely, Figs. 2(a) and 3(a) illustrate the incident, reflected, and transmitted spectra and Figs. 2(b) and 3(b) show the squared modulus of the electric field $|E(X, 0, Z)|^2$ in the (X, Z) plane.

For a 10-μm incident beam waist [Fig. 2(a)], the incident spectrum is quite peaked about $\theta_m = 41.6°$, corresponding to the maximum of transmission of this microcavity. The transmitted spectrum shape seems almost unchanged compared with the incident spectrum, although the reflected spectrum shows a slight dip that indicates that the various PW's that constitute the incident spectrum are unequally reflected by the microcavity. This effect is much more dramatic in Fig. 3(a) for $w = 1\ \mu$m. In this case the strongly focused beam shows a broad incident spectrum that ranges from 30° to 55°. In this situation most of the light is reflected by the microcavity, and the transmitted beam corresponds only to the center of the incident PW spectrum, leading to a sharp dark line in the reflected spot. This filtering effect comes from the angular transmission window of the microcavity and can have important consequences for the total field that takes place in the microcavity spacer, as we now discuss.

Figure 2(b), which corresponds to $w = 10\ \mu$m, shows an amplification of 16.8 compared with the incident maximum, whereas Fig. 3(b), which corresponds to $w = 1\ \mu$m, reaches only 1.15. In other words, the strongly focused pump beam of Fig. 3 cannot enter the cavity and is almost totally reflected by the microstructure.

In addition, it is interesting to note that lateral extent of the beam is strongly altered inside the microcavity spacer. Figures 2(b) and 3(b) show that the internal lateral size L_{cav} of the beam along the X axis and in the
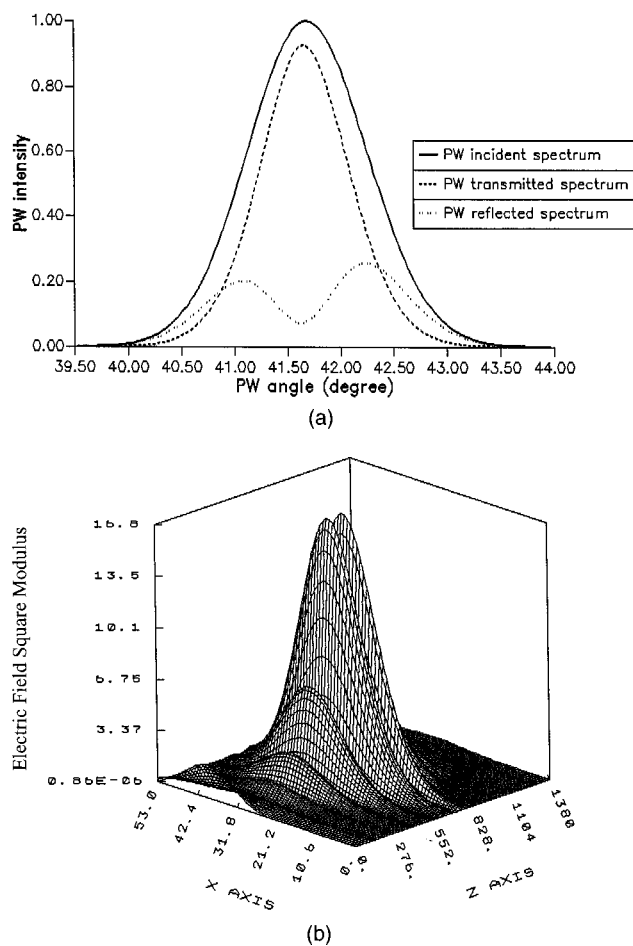
(a)

(b)

Fig. 2. Pump waist, 10 μm. (a) Incident, reflected, and transmitted PW spectrum, (b) squared modulus of the electric field in the sample (X, Z) plane (X and Z axes are graduated in micrometers). The vertical axis is normalized to the incident field.

plane of maximum electric field inside the cavity is 16.4 μm when $w = 10$ μm and is as large as 5.9 μm when $w = 1$ μm. Here again, this lateral spreading comes from the strong filtering effect of the microstructure, especially for $w = 1$ μm.

To confirm experimentally some of the previous calculations, we now investigate the luminescence of Pr ions located inside the spacer of the microcavity when it is pumped with focused beams with 5- or 1-μm beam waists. As indicated above, the luminescence is studied at $\lambda_0 = 490$ nm, whereas $\lambda_p = 457.9$ nm is the pump beam wavelength (TE polarization). Because of the microcavity, the luminescence is strongly peaked about the direction normal to the layer, and our detection system can easily collect 100% of the fluorescence light that escapes the structure in the upper or the lower semi-infinite air media that surround the microstructure. Figure 4 shows the recorded Pr-emitted luminescent power in the upper semi-infinite air space versus pump power P_c inside the microcavity when the pump beam waist is $w = 5$ μm (open circles) or $w = 1$ μm (crosses). The effective pump power inside the microcavity P_c (Fig. 4) is calculated according to

$$P_c = \frac{1}{2} n_H Y_0 \int\int |E(X, y, Z_m)|^2 \mathrm{d}X \mathrm{d}y, \qquad (5)$$

where Z_m is the plane of maximum electric field. Experimentally, the recorded luminescence power in air, P_L, corresponds to 14% of the total power emitted by the Pr ions.[5]
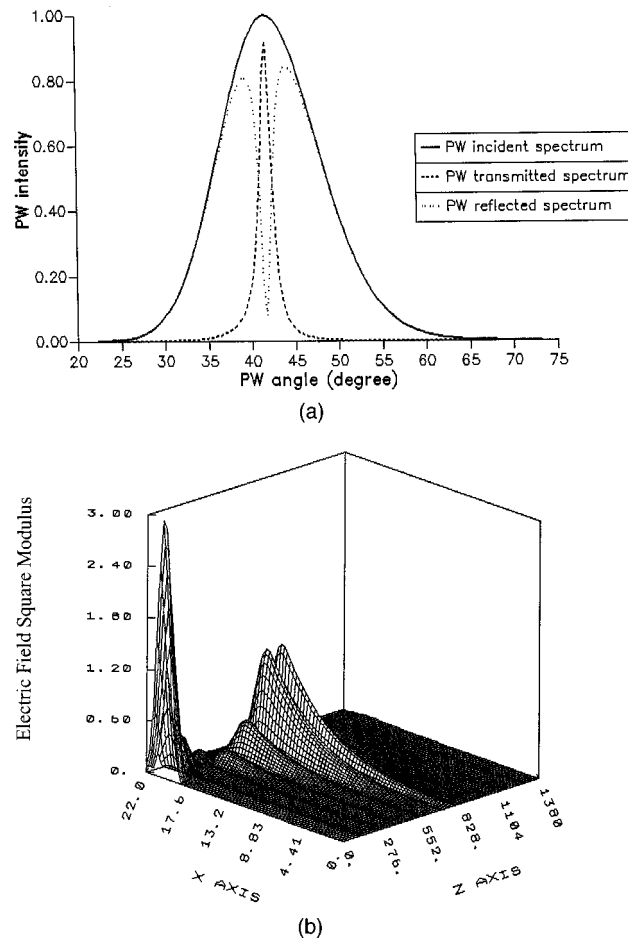

(a)

(b)

Fig. 3. Pump waist, 1 μm. (a) Incident, reflected, and transmitted PW spectrum, (b) squared modulus of the electric field in the sample (X, Z) plane (X and Z axes are graduated in micrometers). The field at $Z = 0$ is the superposition of the incident and the reflected fields and has thus a modulus greater than 1.
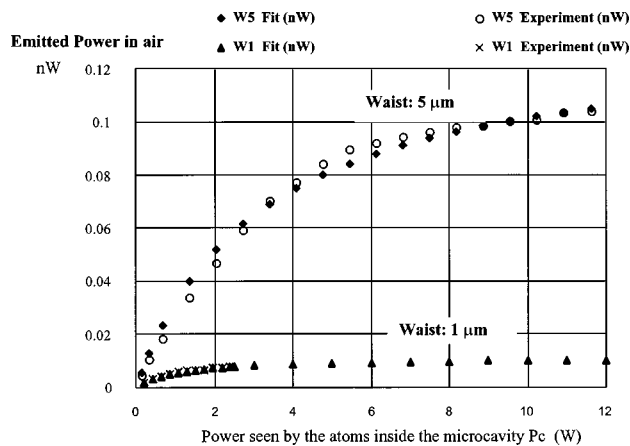

Fig. 4. Pr emitted power (in nanowatts) in the upper semi-infinite air space versus effective pump power P_c (in watts) seen by the atoms inside the microcavity.

To fit the data we model the Pr ions as three-level atoms (with two excited states and a rapid relaxation between them) and approximate the laser beam as an effective cylinder with area S_0. Then P_L is given by

$$P_L = \hbar \omega \Gamma_r s S_0 \frac{P_c}{P_c + S_0 \hbar \omega \Gamma_{\text{tot}}/\Sigma}, \qquad (6)$$

where s is the surface density of the implanted Pr ions, S_0 is the illuminated area, Σ is the pump absorption cross section, Γ_r is the radiative decay rate to the ground state, and $\Gamma_{\text{tot}} = \Gamma_r + \Gamma_{nr}$ is the total decay rate to the ground state, which is the sum of the radiative and the nonradiative contributions. Modeling the pump laser as a truncated Gaussian gives a slightly different functional form but displays the same saturation behavior. Depending on the microcavity power P_c, two regimes can be distinguished:

Linear Regime: $P_c \ll (S_0 \hbar \omega \Gamma_{\text{tot}})/\Sigma$. Here $P_L = s(\Gamma_r/\Gamma_{\text{tot}})\Sigma P_c$, so the luminescence power depends not on the effective area of the pump beam but only on the total pump power coupled into the cavity. We find experimentally that $P_L^{5\,\mu\text{m}}/P_L^{1\,\mu\text{m}} = P_c^{5\,\mu\text{m}}/P_c^{1\,\mu\text{m}} \approx 5$, in good agreement with the calculated power inside the microcavity given by Eq. (5). This results show clearly that the strong spatial filtering effect leads to a microcavity power P_c that is five times stronger for the 5-μm beam waist than for the 1-μm beam.

Saturation Regime: $P_c \gg (S_0 \hbar \omega \Gamma_{\text{tot}})/\Sigma$. In the saturation limit we have $P_L = \hbar \omega s S_0 \Gamma_r$. Inasmuch as all atoms are saturated, the luminescence power depends not on the total pump power but only on its effective area S_0. Experimentally we find that $P_L^{5\,\mu\text{m}}/P_L^{1\,\mu\text{m}} = S_0^{5\,\mu\text{m}}/S_0^{1\,\mu\text{m}} \approx 9$. This result can be explained simply, because the calculated area of excited atoms is ~ 5.9 μm^2 for $w = 1\,\mu\text{m}\,(L_{\text{cav}} = 5.9\,\mu\text{m})$ and $\sim 52.5\,\mu\text{m}^2$ for $w = 5\,\mu\text{m}\,(L_{\text{cav}} = 10.5\,\mu\text{m})$. We find therefore a calculated active surface ratio $S_0^{5\,\mu\text{m}}/S_0^{1\,\mu\text{m}} = 8.9$ in the cavity spacer, in good agreement with the measured luminescence power ratio of 9. By fitting Eq. (6) with the experimental curves it is also possible to obtain an estimate of the absorption cross section. Our cylindrical laser beam model gives $\Sigma = 5 \times 10^{-20}$ cm^2, in reasonable agreement with other published values.[9]

In conclusion, we have presented some theoretical and experimental results concerning strong focusing inside planar microcavities when the incoming wavelength λ_p is blueshifted compared with the resonance wavelength λ_0 at which the cavity is tuned to normal incidence. Using the luminescence of Pr ions implanted inside the microstructure as a microscopic probe for the total electric field inside the cavity, we have demonstrated that strong focusing is not necessarily associated with an enhancement of the Pr ion's pumping efficiency. More precisely, in spite of the reduction of the illuminated area, the incoming beam is strongly spatially filtered, leading to a decrease in the overall pump intensity seen by the luminescent ions inside the microcavity. These results may have important consequences in the study of the spectroscopy of a single molecule located in a microcavity. In this case a focused pump beam usually discriminates spatially the location of the single active molecule in addition to providing the excitation power.[10] More generally, these focusing problems can be encountered in any photonic structure that exhibits sharp electromagnetic resonances, such as microcavities in photonic bandgap materials.[11]

REFERENCES

1. F. DeMartini, G. Innocenti, G. R. Jacobivitz, and P. Mataloni, "Anomalous spontaneous emission time in a microscopic optical cavity," Phys. Rev. Lett. **59**, 2955–2958 (1987).
2. H. Yokoyama, M. Suzuki, and Y. Nambu, "Spontaneous emission and laser oscillation properties of microcavities containing a dye solution," Appl. Phys. Lett. **58**, 2598–2600 (1991).
3. G. Björk, S. Machida, Y. Yamamoto, and K. Igeta, "Modification of spontaneous emission rate in planar dielectric microcavity structures," Phys. Rev. A **44**, 669–681 (1991).
4. E. F. Shubert, A. M. Vredenberg, N. E. J. Hunt, Y. H. Yong, P. C. Becker, J. M. Poate, D. C. Jacobson, L. C. Feldman, and G. J. Zydzik, "Giant enhancement of luminescence intensity in Er-doped Si/SiO$_2$ resonant cavities," Appl. Phys. Lett. **61**, 1381–1383 (1992); A. M. Vredenberg, N. E. J. Hunt, E. F. Shubert, D. C. Jacobson, J. M. Poate, and G. J. Zydzik, "Controlled atomic spontaneous emission from Er^{3+} in a transparent Si/SiO$_2$ microcavity," Phys. Rev. Lett. **71**, 517–520 (1993).
5. H. Rigneault, S. Robert, C. Begon, B. Jacquier, and P. Moretti, "Radiative and guided wave emission of Er^{3+} atoms located in planar multidielectric structures," Phys. Rev. A **55**, 1497–1502 (1997).
6. H. Rigneault, F. Flory, S. Monneret, S. Robert, and L. Roux, "Fluorescence of Ta$_2$O$_5$ thin films doped by kilo-electron-volt Er implantation: application to microcavities," Appl. Opt. **35**, 5005–5012 (1996).
7. S. Monneret, S. Tisserand, F. Flory, and H. Rigneault, "Light-induced refractive-index modifications in dielectric thin films: experimental determination of relaxation time and amplitude," Appl. Opt. **35**, 5013–5020 (1996).
8. S. Monneret, "Coupleur à prisme à deux faisceaux pour la caractérisation d'effets non linéaires thermiques dans les couches minces," Ph.D. dissertation (University Aix-Marseille III, Marseille, France, 1996).
9. W. Seeber, E. A. Downing, L. Hesselink, M. M. Fejer, and D. Ehrt, "Pr^{3+}-doped fluoride glasses," J. Non-Cryst. Solids **189**, 218–226 (1995).
10. F. DeMartini, G. Di Giuseppe, and M. Marrocco, "Single mode generation of quantum photon states by excited single molecules in a microcavity trap," Phys. Rev. Lett. **76**, 900–903 (1996).
11. P. Villeneuve, S. Fan, and J. D. Joannopoulos, "Microcavities in photonic crystals: mode symmetry, tunability, and coupling efficiency," Phys. Rev. B **54**, 7837–7842 (1996).